

Article

Urban Growth Modeling and Land-Use/Land-Cover Change Analysis in a Metropolitan Area (Case Study: Tabriz)

Hassan Mahmoudzadeh ^{1,*}, Asghar Abedini ² and Farshid Aram ^{2,*}¹ Department of Geography and Urban Planning, University of Tabriz, Tabriz 5166616471, Iran² Urban Planning Department, Urmia University, Urmia 5756151818, Iran

* Correspondence: mahmoudzadeh@tabrizu.ac.ir (H.M.); farshid.aram@alumnos.upm.es (F.A.)

Abstract: During the last three decades, the expansion of the Tabriz Metropolitan Area (TMA) to the surrounding areas has caused the destruction of environmental resources and problems such as disturbing ecological balance, increasing service costs, construction over unsuitable lands, exacerbation of air pollution, and lack of consideration of existing deteriorated textures and previous ongoing trends, reducing the environmental quality of the TMA. The goal of this study was to perform ecological modeling of urban development in the TMA with respect to the preservation of environmental resources, prevention of urban sprawl, and the management of the physical expansion of the TMA in an eco-friendly manner. In this research, to investigate the previous pattern of growth of the TMA, Landsat satellite imagers from 1984 to 2018 were used to discover the non-ecological and sprawl development of the TMA, and artificial neural networks and logistic regression techniques were applied to simulate future development up to 2038. According to information from the Iranian Statistical Center and 34 year of satellite imagery analysis, the population of the TMA increased from 1,007,992 to 1,961,560 during this period. Additionally, urban and rural land area increased from 7220.34 hectares to 27,640.57 hectares. A lack of coordination between population and urban expansion, as well as a decrease of 8513.61 hectares of agricultural and garden lands was inferred from the Holdern model. Detailed Calculations of the Holdern index (sprawl tendency) showed a lack of consideration of urban development capacity with population growth rate, and the Holdern index is equal to 0.6 in Tabriz. For future ecologic development of the TMA, hexagonal blocking of the urbanization probability map was used alongside environmental development policies in the form of using 30 percent of infill development capacities of inefficient land uses to prevent sprawl growth in Tabriz. Additionally, to preserve ecological landscapes, ecological networks in the form of green belts and bows with a length of 91 km were designed that may be effective in preventing the merging of small cities and nearby villages in the Tabriz metropolis.

Keywords: land use changes; ecologic development; Tabriz Metropolitan Area (TMA); artificial neural networks; logistic regression; urban planning



Citation: Mahmoudzadeh, H.; Abedini, A.; Aram, F. Urban Growth Modeling and Land-Use/Land-Cover Change Analysis in a Metropolitan Area (Case Study: Tabriz). *Land* **2022**, *11*, 2162. <https://doi.org/10.3390/land11122162>

Academic Editors: David Pastor-Escuredo, Alfredo J. Morales and Yolanda Torres

Received: 16 October 2022

Accepted: 25 November 2022

Published: 30 November 2022

Publisher's Note: MDPI stays neutral with regard to jurisdictional claims in published maps and institutional affiliations.



Copyright: © 2022 by the authors. Licensee MDPI, Basel, Switzerland. This article is an open access article distributed under the terms and conditions of the Creative Commons Attribution (CC BY) license (<https://creativecommons.org/licenses/by/4.0/>).

1. Introduction

Changes in land use and land cover are regarded as humanity's most noticeable impact on the environment [1]. Supplying the requirements of an increasing population has led to significant changes to the surface of the Earth, with undesirable effects from local to global scales [2]. Decision makers and urban planners need accurate and comprehensive data on prospective urban growth to evaluate new development requirements, their location and features, and the effects of urban development before and after project implementation [3]. Modeling spatial land-use transition can lead to improved knowledge of the environmental and Socio-economic variables relevant in promoting urbanization trends [4]. Many researchers have investigated the adverse effects of urban expansion, such as reducing natural areas and habitat fragmentation [5–8]; impacts on biodiversity [9,10]; deforestation [11–13]; increasing air, water, and soil pollution [14–16]; exacerbating hydrological

problems [17,18]; disturbing natural environments and wildlife [19,20]; and regional and global warming and climate change [21,22]. Interest in land-use change modeling has increased rapidly in recent years [3], and an increasing number of academics are attempting to explore the urban development process using various techniques, including cellular automata [23,24], agent-based models [25–27], artificial neural networks [28–32], Markov chain [33–37], and support vector machine [38–41]. With respect to a comprehensive view of changes occurring large areas from an environmental perspective, many studies have such changes in areas such as the Greater Accra Metropolitan Area, Ghana [42], Addis Ababa, Ethiopia [43], the Chennai Metropolitan area, India [44], the Semarang Metropolitan Region, Indonesia [45], the Lagos Metropolitan Region, Nigeria [46], the Yangtze River Middle Reaches Megalopolis, China [47], Metropolitan Guangzhou, China [48], Lucknow Metropolitan Area, India [49], Tehran Metropolitan Region, Iran [50], Atlanta Metropolitan Area, USA [51], the Pune Metropolitan Region, India [52], the Kathmandu Metropolitan Region, Nepal [53], and the Santiago Metropolitan Area, Chile [54].

The Innovation of this paper is in the simultaneous use of two logistic regression and LTM models to predict urban development and determine a framework for the ecological development of the TMA. Therefore, the purpose of this study is to conduct a comprehensive survey of the status of urban development in one of the most significant metropolitan areas of Iran from an environmental perspective and provide applicable solutions to preserve valuable green land from urban development.

2. Methodology

2.1. Study Area

The Tabriz Metropolitan Area is located in the northwest of Iran and lies approximately between latitudes $38^{\circ}11' N$ and $38^{\circ}16' N$ and longitudes $45^{\circ}56' E$ and $46^{\circ}38' E$, with a territory of 220,705 hectares includes the 9 cities of Tabriz, Sofian, Khajeh, Basmang, Sardrood, Khosrowshahr, Sahand, Ilkhchi, and Usko, as well as 72 villages that cover 4.81% of the total area of East Azarbaijan province (Figure 1). It is bounded by the Sahand mountain range on the south and west, Urmia Lake on the east, and the Mishadagh highlands to the north. The TMA is one of the most populous and fastest-growing urban areas in Iran. According to the Iranian Census Bureau, the population of the TMA in 1984 was 1,007,992 and has since increased, with a population of 1,961,560 in 2018, which makes it the fast-growing city in the past 34 years. Tabriz, as a central city of the TMA has a high concentration of administrative, commercial, and industrial functions. The adjacent cities and villages of Tabriz have potential for merging into the main body of the Tabriz metropolis. The present conditions make it essential to consider modeling the urban growth of the TMA in order to prevent urban sprawl and the destruction of high-quality agricultural and garden land.

2.2. Methods

The methodology of this study is based on the evaluation of LULC change analysis and urban growth prediction of the Tabriz Metropolitan Area using remote sensing data and logistic regression and ANN methods, as shown in Figure 2, which will be discussed in detail in the following sections. In this study, the following dataset was used in the urban modeling of the TMA: land-use maps of 1984, 2000, and 2018 were derived using 30 m resolution satellite images from Landsat 5 TM, Landsat 7 ETM+, and Landsat OLS, respectively (Table 1), and Google Earth was used for the validation of land-use maps of the TMA for the study periods, along with field knowledge. Images from 1985, with the ability to show historical imagery of Google earth pro and the appropriate zoom, are available in high resolution, and changes in urban development and vegetation cover are easily accessible through the provided timeline. The selected images had the most time matching with the official demographic data of the Tabriz Metropolitan Area. From a practical point of view, the changes that have taken place in the LULC are traceable by the reduction in natural land cover, such as agricultural and garden lands, by the expansion of built-up

land uses. In this study, ENVI 5.3 software was used to prepare land-use maps, Terrset 2020 software was used to prepare urbanization probability maps, LTM software was used for artificial neural networks, IBM SPSS Statistics 20 was used for statistical analyses, and ArcMap 10.6.1 was used for layouts.

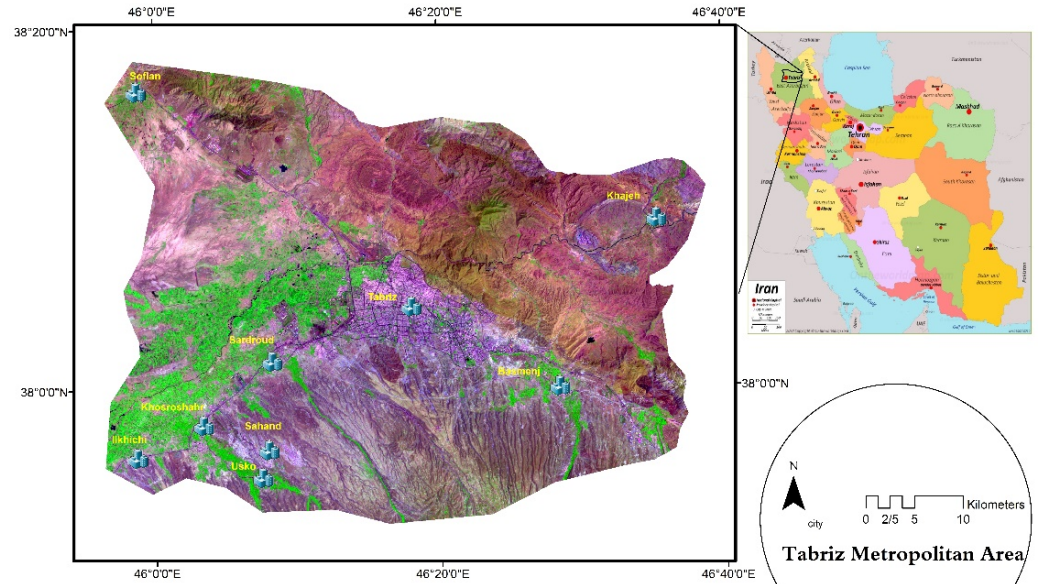


Figure 1. Study area: Tabriz Metropolitan Area, East Azarbiajan, Iran.

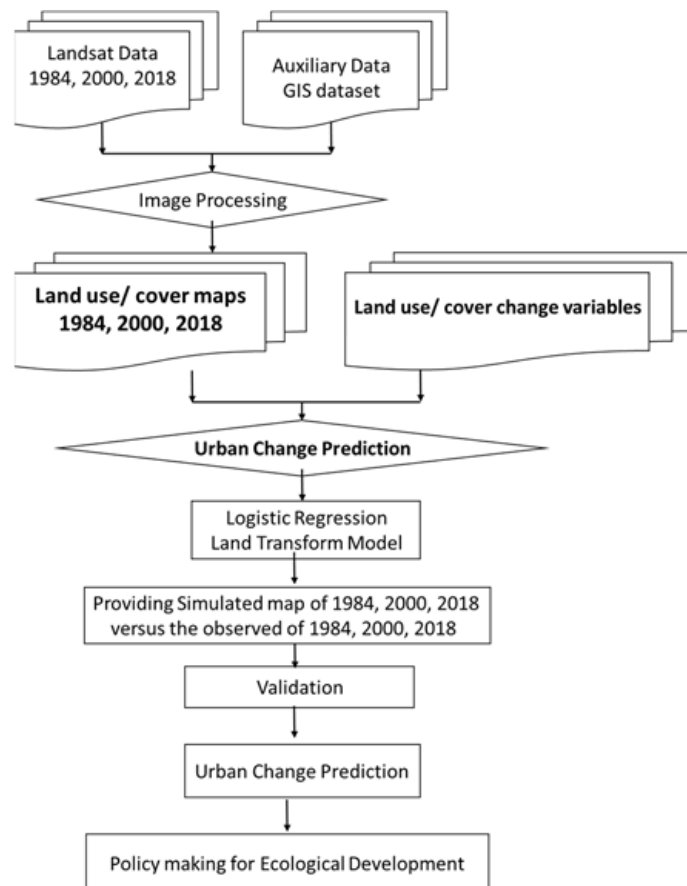


Figure 2. Flow chart of the presented methodology.

Table 1. Characteristics of remote sensing data.

Data	Source	Resolution (m)	Date
Landsat 5 TM	US Geological Survey	30	10 July 1984
Landsat 7 ETM+	US Geological Survey	30,15 (PAN)	31 August 2000
Landsat 8 OLI	US Geological Survey	30,15 (PAN)	8 July 2018

Only one scene in the current study had pass-row 168-34 and less than 10% cloud cover in all scenes. Mosaicking and color balancing were not necessary because only one scene was used. As level 1 was used, only standard radiometric correction and quick atmospheric correction (QUAC) were performed using Envi software. The Landsat Gap Fill plugin (for SLC-OFF images) in Envi software was used to correct this error.

Auxiliary GIS datasets were derived from the Iran National Cartographic Center and GIS analysis, covering factors such as slope, population density, distance from major roads, distance from urban centers, distance from power lines, distance from rivers, distance from faults, number of urban cells different from the center cell in each 7×7 neighborhood, geology, barren lands, garden lands, distance from industrial centers, distance from medical centers, distance from cultural centers, distance from administrative centers, distance from recreational centers, distance from CBDs, elevation, the distribution of land prices, etc.

Land-Use/Land-Cover Change Detection

Multitemporal Landsat satellite images were used to prepare LULC maps for the observation years using eCognition Developer software based on a nearest-neighbor classifier in six major classes: barren lands, built-up lands, agricultural lands, garden lands, pasture land, and water bodies. A brief description the satellite data and major LULC classes used in this study is provided in Table 2. As shown in Figure 3, urban expansion occurred mostly along the borders of existing urban areas; therefore, the proximity to urban facilities seems to play a significant role in urban development.

Table 2. Land use quantitative and structural changes in the TMA, 1984–2018 (unit: Ha).

Land Use	1984		2000		2018		1984–2000	2000–2018	1984–2018
	Area	Total%	Area	Total%	Area	Total%	Variation	Variation	Variation
Barren lands	151,962.57	68.85	149,223.51	67.60	147,051.99	66.62	−1.80	−1.46	−3.23
Built-up lands	7220.34	3.27	14,027.58	6.35	22,346.82	10.12	94.27	59.30	209.50
Agricultural lands	25,369.83	11.49	23,259.42	10.53	22,489.02	10.18	−8.32	−3.31	−11.36
Garden lands	10,242.63	4.65	9094.86	4.12	6653.43	3.01	−11.21	−26.84	−35.04
Pasture lands	25,248.15	11.44	24,669.99	11.17	21,583.80	9.77	−2.29	−12.51	−14.51
Water bodies	669.24	0.30	437.40	0.19	587.700	0.26	−34.64	34.36	12.18

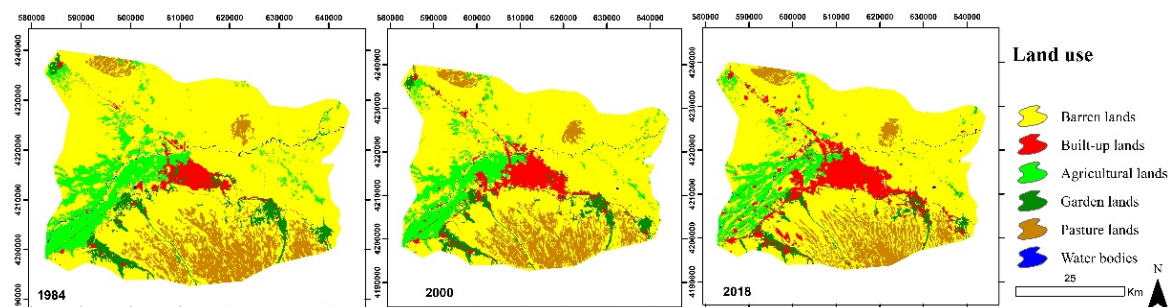
**Figure 3.** LULC classes derived from Landsat data for the TMA.

Table 2 shows that the area of built-up lands increased from 7220 hectares in 1984 to 22,346 hectares in 2018; thus, the percentage of changes was 209.49%. The area of garden lands was reduced from 10,242 hectares to 6653 hectares, corresponding to a percentage change of −35.04% (Table 2).

The overall accuracy and kappa coefficient based on the ground truth region of interest are listed in Table 3.

Table 3. Overall accuracy and kappa coefficient in three classified images.

	1984	2000	2018
Overall Accuracy	93.6	95.3	96.4
Kappa Coefficient	0.89	0.91	0.94

For improved visualization of changes in urban expansion, the built-up areas based on nine city boundaries were compared with population changes by overlaying radar diagrams on the DEM map of the TMA. The results show the changes in the area of cities of the TMA have occurred faster than four times the changes in population and urban sprawl, as evidenced by the irregular growth of cities on garden lands in and around the cities (Figure 4).

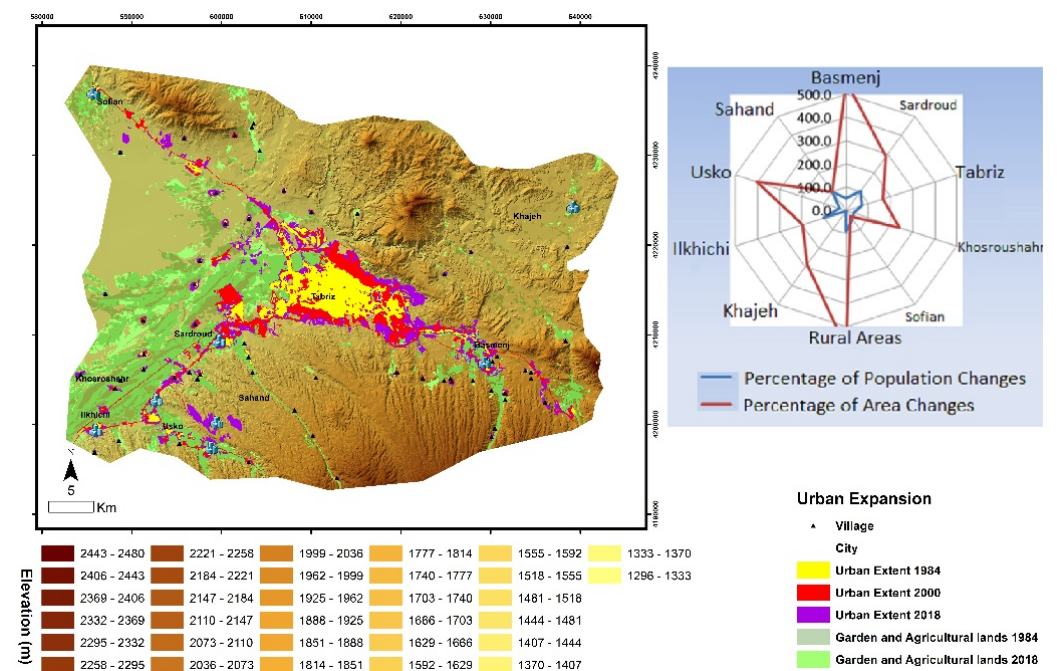


Figure 4. Urban expansion trend in the TMA from 1894 to 2018 on a DEM.

2.3. Logistic Regression Model

Logistic regression is mainly used to model a binary (0, 1) variable based on one or more other variables called predictors [55]. This model has been widely used in studies and simulations of the driving forces of urban expansion [56]. A discrete logistic regression method was used in the present work to estimate the contribution of influencing factors to urban expansion. The model sets the dependent variable (Y) as 1 when urban expansion occurs (otherwise, Y is equal to 0); therefore, the logistic regression and its value can be determined with the following formula [57]:

$$P(y = 1|X) = \frac{\exp(\sum BX)}{1 + \exp(\sum BX)} \tag{1}$$

where P is the probability of the dependent variable; X defines the independent variables as $X = (x_0, x_1, x_2, \dots, x_k), x_0 = 1$; and B represents the calculated parameters, i.e., $B = (b_0, b_1, b_2, \dots, b_k)$.

In order to linearize the above equation and eliminate the 0/1 boundaries for the original dependent variable, which is the probability, the following transformation is usually applied:

$$P' = \ln\left(\frac{P}{1-P}\right) \quad (2)$$

This transformation is related to the logit transformation. Therefore, after the transformation, P' can logically assume any value between plus and minus infinity [58]. The logit transformation of binary data guarantees that the dependent variable will be continuous, and the new dependent variable (logit transformation of the probability) is limitless. Furthermore, this guarantees that the probability layer will be continuous within the range of 0 to 1. By implementing the logit transformation on both sides of the logit regression model mentioned, we extracted a generic linear regression model:

$$\ln\left(\frac{P}{1-P}\right) = b_0 + b_1 \times 1 + b_2 \times 2 + \dots + b_k \times k + \varepsilon \quad (3)$$

A set of predictor variables was chosen based on preliminary research, with non-correlated characteristics as independent variables, along with the dependent variable of urban growth from 1984 to 2018 in the logistic regression model (Table 4 and Figure 5).

The conditional probability of each regression model when the dependent variable is one was obtained, and the spatial distribution of the likelihood of built-up urban lands expansion in the TMA between 1984 and 2018 in three periods was simulated by TerrSet software (Figure 6).

Table 4. List of variables as inputs for logistic regression and LTM.

Variable Description	Source and Description	Nature of Variable
Dependent variable Urban growth from 1984 to 2018	Subtraction of the Boolean Urban areas for 1984 from 2018 (classified images); 0—no urban growth; 1—urban growth	Dichotomous
Slope	<i>Slope</i> in percent	Continuous
Population density	Population density (person/ha)	Continuous
Distance from commercial centers	Euclidean distance from CBD(m)	Continuous
Distance from roads	Distance to the nearest major road (m)	Continuous
Distance from urban centers	Euclidean distance to the urban region (m)	Continuous
Distance from power lines	Euclidean distance from power lines (m)	Continuous
Distance from rivers	Euclidean distance from rivers (m)	Continuous
Distance from faults	Euclidean distance from faults (m)	Continuous
Urban CVN (center versus neighbor)	Number of urban cells within a 7 · 7 cell window (ranging from 0 to 8)	Ranging from 0 to 8
Geology	The degree of hardness for lithological structures	Continuous
Barren lands	1—bare land; 0—not bare land	Design
Garden lands	1—garden land; 0—not garden land	Design
Agriculture lands	1— <i>agriculture</i> land; 0—not <i>agriculture</i> land	Design
Pasture lands	1—pasture land; 0—not pasture land	Design
Built up lands	1— <i>built-up lands</i> ; 0—not built-up lands	Design
Distribution of land price	Spatial distribution of land price	Continuous

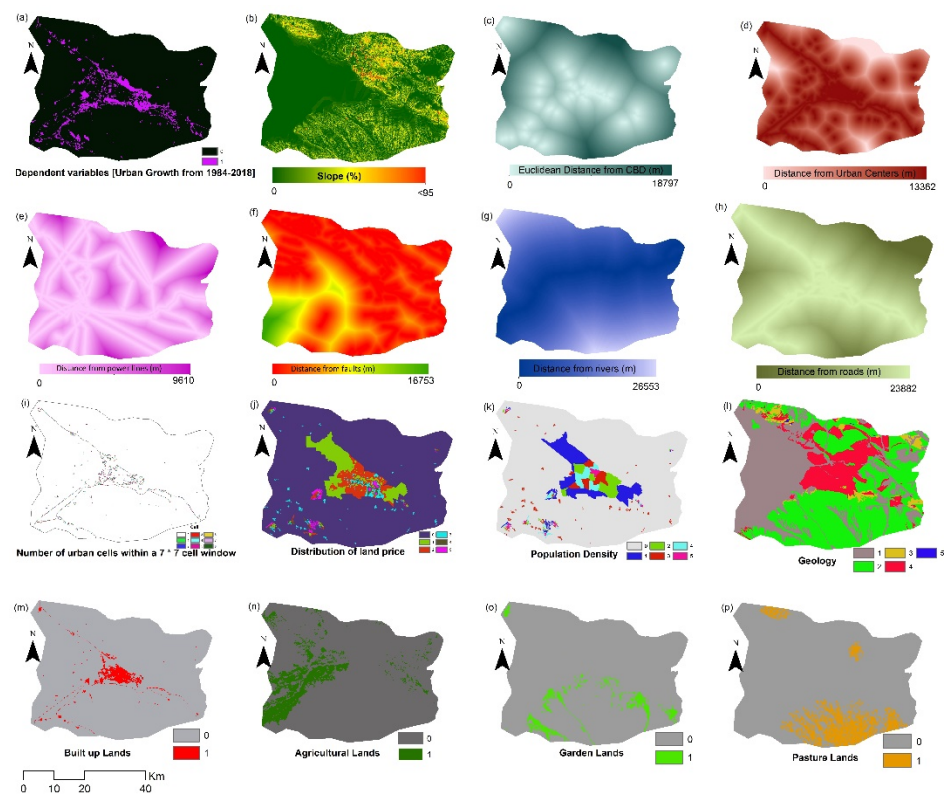


Figure 5. Raster layers of independent variables. (a). dependent variable (urban growth 1984 to 2018), (b). slope(percent), (c). distance from CBD (m), (d). distance from urban centers (m), (e). distance from power lines (m), (f). distance from faults (m), (g). distance from rivers (m), (h). distance from roads(m), (i). distance from rivers (m), (j). number of urban cells within a 7 · 7 cell window, (k). distribution of land price, (l). Geology, (m). Built up lands, (n). agricultural lands, (o). garden lands, (p). pasture lands.

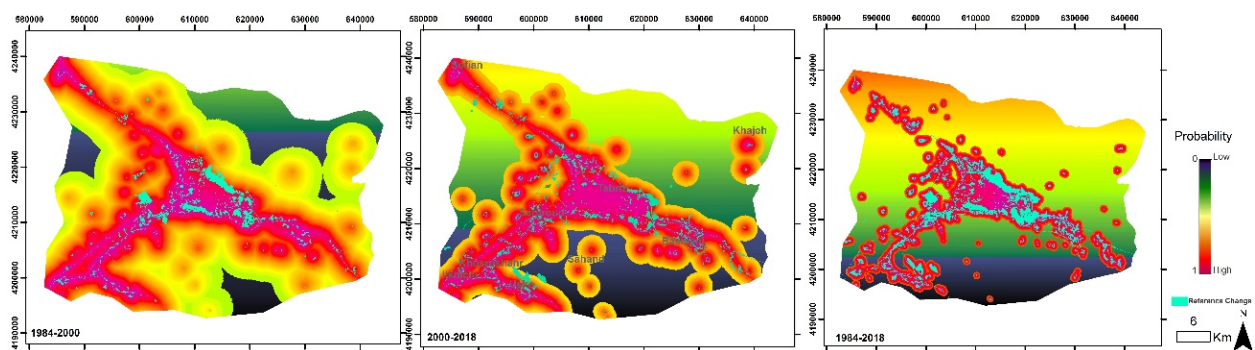


Figure 6. Urban growth probability maps of the TMA in three periods based on LR data.

As shown in Figure 6, the high-probability urbanization cores are mainly located along main roads and are connected to previous urban centers. Non-connected centers away from cities indicate the possibility of rural area development, which increases the likelihood of growth in the vicinity of the main core of cities. Urban change maps were nominal as a dependent variable in the LR model in the preparation of the urbanization probability map. Furthermore, the independent variables in the mentioned model were converted to a normal form in order to calculate R2 indices.

Results

Validation is an important process that allows users to understand the accuracy of the prediction model [44]. Relative operating characteristic (ROC) has been used to validate the logistic regression model [59]. The following formula defines the ROC to calculate a model’s accuracy:

$$ROC = \sum_{i=1}^n [x_{i+1} - x_i] \cdot [y_i + (y_{i+1} - y_i)/2]; \tag{4}$$

where x_i is the rate of false positives for threshold i , y_i is the rate of true positives for threshold i , and $n+1$ is the number of thresholds. ROC is an excellent statistic for measuring the goodness of fit of logistic regression. An ROC value of 1 indicates perfect spatial agreement between the actual urban growth map and the predicted probability map. The ROC value ranges from 0 to 1, where 1 indicates a perfect fit, and 0.5 indicates a random fit. The larger the ROC value, the better the fit [60]. Another index used to validate the predicted model is R-squared, i.e., the square of the correlation between the model’s projected values and the actual values. This correlation can range from -1 to 1 , and the square of the correlation ranges from 0 to 1. The higher the magnitude of the correlation between the projected values and the actual values, the greater the R-squared, regardless of whether the correlation is positive or negative.

$$\text{Pseudo R-Squared} = (\log(\text{Likelihood})/\log(L0)) \tag{5}$$

where $L0$ is the value of the likelihood function if all coefficients except the intercept are 0 [61]. The fit of a logistic model with a dataset can be evaluated using pseudo-R2 measures. The pseudo-R2 value, which indicates the logit model/dataset fit, ranges from 0 (no relationship) to 1 (perfect fit). A value greater than 0.2 for the pseudo-R2 shows a relatively good fit [62]. The ROC and R² indices shown in Table 5 demonstrate the good fit between the referenced and real urban growth in three periods.

Table 5. Model validation results in terms of ROC and pseudo-R² for the probability map.

1984–2000		2000–2018		1984–2018	
ROC	Pseudo-R ²	ROC	Pseudo-R ²	ROC	Pseudo-R ²
0.86	0.78	0.82	0.74	0.89	0.79

Model validation results show that the urban development probability pattern maps were obtained with values of more than 0.8 for ROC and 0.7 for pseudo-R², indicating that the independent variables used to simulating urban development were well-selected. For sensitivity analysis in this study, the logistic regression model was rerun after eliminating one of one the independent variables from the full set of variables and recording acquired ROCs for the 1984–2018 period. The advantage of this procedure is in the sensitivity of the variables and discovery of the effect of variables in the final model. As shown in Figure 7, the variables distance from urban centers, population density, number of urban cells in a 7 × 7 window, slope, and distance from roads have the most impact on the urbanization process in the TMA. (Figure 7)

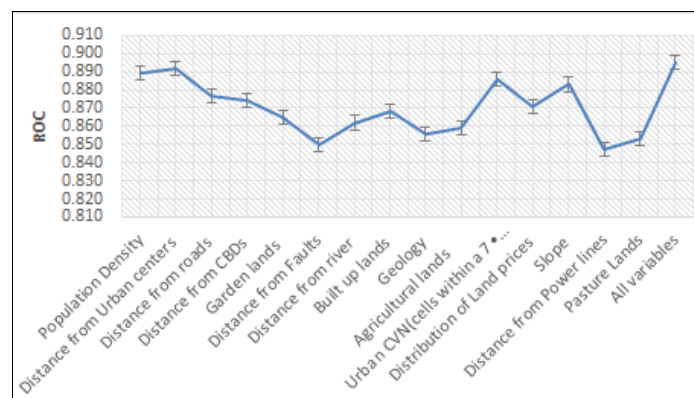


Figure 7. Sensitivity analysis of the logistic regression model by the elimination of independent variables for the 1984–2018 period with ROC fluctuation.

The coefficients of the regression function permit an assessment of the relative importance of the independent variables. Those independent variables that can explain the dependent variable are represented by the value of the Cox and Snell R² (0.39), as well as the Nagelkerke R² (0.61) (Table 6).

Table 6. Model summary statistics.

Step 14	−2 Log Likelihood	Cox & Snell R ²	Nagelkerke R ²	Pseudo R ²
	26391.79	0.39	0.61	0.79

All independent variables except pasture lands, distance from power lines, geology, and distance from rivers were significant at the 0.05 level. The factors of distance from urban centers, population density, urban CVN (center versus neighbor), slope, distance from roads, distance from CBDs, and distribution of land prices had a positive effect on urban growth. Distance from urban centers made the largest contribution. These results indicate that urban growth in the TMA was mostly dependent on proximity to previous urban centers with a high concentration of facilities, reflecting the characteristics of urban growth during the period from 1984 to 2018 (Table 7).

Table 7. Logistic regression model results.

	B ^a	S.E. ^b	Wald ^c	Df ^d	Sig. ^e	Exp(B) ^f	95% C.I. for EXP(B) ^g	
							Lower	Upper
Constant	−2.867	0.030	8861.936	1	0.000	0.507		
Built-up lands	−0.26	0.011	6.178	1	0.000	0.974	0.954	0.994
Agriculture lands	−0.80	0.012	45.186	1	0.000	0.924	0.902	0.945
Land prices	−0.155	0.021	53.915	1	0.000	0.856	0.822	0.893
Pasture lands	−0.137	0.010	183.715	1	0.013	0.872	0.855	0.890
Garden lands	−0.131	0.010	180.805	1	0.000	0.877	0.861	0.894
Dist f roads	0.328	0.010	1067.199	1	0.000	1.389	1.362	1.416
Dist f urban	1.519	0.050	922.745	1	0.000	0.219	0.199	0.242
Dist f CBDs	−0.206	0.017	147.599	1	0.000	0.814	0.788	0.842
Dist f power lines	−0.39	0.012	10.334	1	0.001	0.962	0.940	0.985
Geology	−0.71	0.011	45.219	1	0.013	0.932	0.913	0.951
Dist f faults	−0.53	0.011	21.772	1	0.000	1.054	1.031	1.077
Urban CVN	0.407	0.013	1028.951	1	0.000	0.665	0.649	0.682
Dist f rivers	−0.057	0.014	17.289	1	0.013	0.944	0.919	0.970
Slope	−0.380	0.029	171.274	1	0.000	0.684	0.646	0.724
Population density	1.105	0.009	13548.603	1	0.000	3.019	2.964	3.076

^a Logistic coefficient. ^b Standard error of estimate. ^c Wald chi-square values. ^d Degree of freedom. ^e Significance. ^f Exponential and coefficient. ^g 95% confidence interval for Exp(B).

2.4. Land Transformation Model

A land transformation model (LTM) is an artificial neural networking mechanism in geographic information systems used to forecast urban growth land uses. The steps of the LTM model include the following procedure (Figure 8):

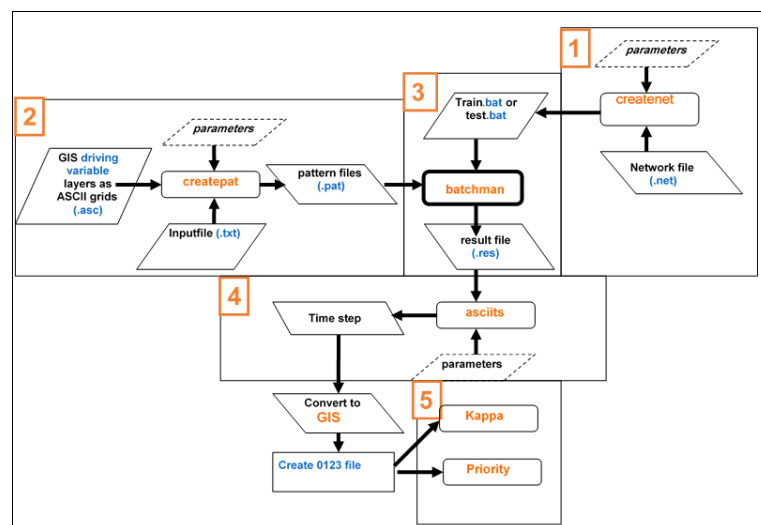


Figure 8. Breakdown of LTM Steps. 1. Create network file: In this step, the drivers prepare for input. The input nodes comprise a number of drivers, the output node always comprise one driver, as it is the final prediction file, and the number of hidden layers is up to the user. 2. Create pattern files: This

step creates the necessary layer for the neural network to recognize which cells it will train on. 3. Batchman_TrainingP: This step starts the NN training and output each 100th cycle. 4. Create GIS-usable files: In this step, each cell that was presented to the network is assigned a number assigned based on the cell’s relationship with the drivers and the urbanization process. Higher numbers represent the neural network’s prediction of a more likely transition of a cell to urban. 5. Assessment of simulation: In this step, the accuracy of the model is calculated based on RMS error, Kappa statistics, and PCM statistics.

Artificial neural networks are a commonly used modeling method with self-adapting, self-organizing, and self-learning abilities, representing the most widely used and effective feed-forward error backpropagation method. A three-layer perceptron ANN structure was adopted to predict urban expansion owing to its simplicity, ease of training and reasonable associative memory, and prediction capabilities [63].

The Land transformation model simulates land-use/cover changes based on socioeconomic and biophysical factors using an artificial neural network (ANN) and a raster GIS modeling environment [30]. The LTM contains six major components: (1) data in a GIS environment, (2) pattern recognition, (3) calibration, (4) model validation, (5) creation of future scenarios of land use, and (6) model outputs and applications within the framework of the GIS [64].

For assessment of the simulation and prediction process, root mean square (RMS), percent correct metric (PCM), and kappa coefficient were calculated according to the following equations:

$$RMS = \frac{1}{N} \sum_{i=1}^N (Pi - Oi)^{1/2} \tag{6}$$

where RMS = root mean square, O_i = original data, P_i = predicted data, and N = number of samples.

$$PCM = \frac{TP}{TCN} \times 100 \tag{7}$$

where PCM = percent correct metric, TP (real change and predicted change) = true positive TCN = transition cell number

$$Kappa = \frac{\left(\left(\frac{TN}{GT}\right) + \left(\frac{TP}{GT}\right)\right) - \left(\left(\left(\frac{SN}{GT}\right) \cdot \left(\frac{RN}{GT}\right)\right) + \left(\left(\frac{SP}{GT}\right) \cdot \left(\frac{RP}{GT}\right)\right)\right)}{1 - \left(\left(\left(\frac{SN}{GT}\right) \cdot \left(\frac{RN}{GT}\right)\right) + \left(\left(\frac{SP}{GT}\right) \cdot \left(\frac{RP}{GT}\right)\right)\right)} \tag{8}$$

- TN = true negative (no real change and no predicted change)
- FN = false negative (no real change but change predicted by the model)
- FP = FALSE POSITIVE (real change but not predicted by the model)
- TP = true positive (real change and predicted change)
- $(SN = TN + FN)$ simulated negative
- $(SP = FP + TP)$ simulated positive
- $(RN = TN + FP)$ real change negative
- $(RP = FN + TP)$ real change positive
- $(GT = TN + FN + FP + TP)$

In this research, the LTM was used for modeling, assuming an equal number of hidden layers and input nodes. Therefore, with the layers mentioned in the logistic regression stage, a network with 15 input nodes, 15 hidden nodes, and one output node was created. The networks in three periods were trained during the training phase with part of the data (one cell per two cells) and tested with the whole dataset in the test phase. The lowest RMS error rate, Kappa coefficient, and PCM in various cycles were stored to produce the urban expression probability map (Table 8). Results show that the model was able to provide urban development trends between 1984 and 2018, and the purple areas in the forecasted maps indicate an optimal match with real change maps in the three periods (Figure 9).

Table 8. Model validation results in ANN based on the LTM model.

	1984–2000		2000–2018			1984–2018			
	RMS		RMS			RMS			
Cycle 9300	Kappa	PCM	Cycle 8600	Kappa	PCM	Cycle 8000	Kappa	PCM	
	0.0197233	0.865437	85.871426	0.0186641	0.853461	86.842313	0.0189534	0.844434	87.831315

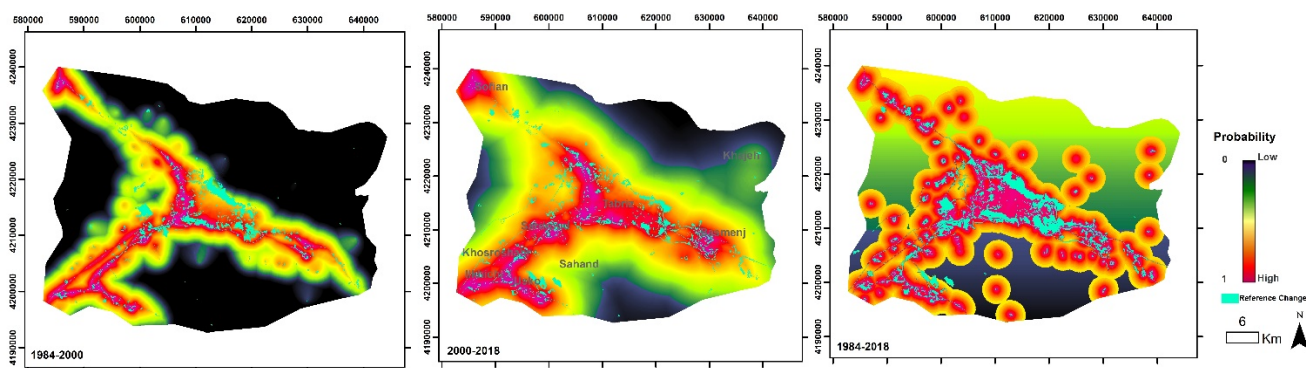


Figure 9. Urban growth probability maps of the TMA during three periods based on LTM data.

Visual interpretation by overlaying of the probability map extracted by artificial Neural network and logistic regression methods shows the agreement of the two maps on the changed areas for the years 1984–2018.

Based on the analysis of the probability of urbanization, the advantages and disadvantages of the ANN-LTM and LR were identified as follows (Tables 9 and 10):

Table 9. Logistic regression advantages and disadvantages.

Advantages	Disadvantages
Logistic regression is easy to implement and interpret and very efficient to train (Terrset).	If the number of observations is less than the number of features, logistic regression should not be used and may lead to overfitting.
It makes no assumptions about distributions of classes in feature the space (Table 4).	It constructs linear boundaries.
It can easily extend to multiple classes (multinomial regression) and a natural probabilistic view of class predictions (lack of necessity).	The major limitation of logistic regression is the assumption of linearity between the dependent variable and the independent variables.
It not only provides a measure of the appropriatenes of a predictor (coefficient size) but also its direction of association (positive or negative) (Tables 6 and 7).	It can only be used to predict discrete functions. Hence, the dependent variable of logistic regression is bound to the discrete number set.
It can rapidly classify unknown records.	Non-linear problems cannot be solved with logistic regression because it has a linear decision surface. Linearly separable data are rarely found in real-world scenarios.
Accuracy on many simple datasets and performs well when the dataset is linearly separable.	Logistic regression requires average or absent multicollinearity between independent variables.
It can interpret model coefficients as indicators of feature importance (Table 7).	It is difficult to obtain complex relationships using logistic regression. More powerful and compact algorithms such as neural networks can easily outperform logistic regression.
Logistic regression is less inclined to overfit, but it can overfit in high dimensional datasets. Regularization (L1 and L2) techniques may be considered to avoid overfitting in such scenarios (Table 6).	In linear regression, independent and dependent variables are related linearly. However, logistic regression requires that independent variables be linearly related to the log odds ($\log(p/(1 - p))$).

Table 10. ANN-LTM advantages and disadvantages.

Advantages	Disadvantages
Can be applied to complex non-linear problems.	It is not known to what extent each independent variable is affected by the dependent variable. Computations are difficult and time-consuming.
Works well with large input data (TMA).	The proper functioning of the model depends on the quality of the training data.
Provides quick predictions after training (Figure 9).	If the model does not work properly, generalization problems arise.
Same accuracy ratio can be achieved, even with small datasets.	

2.5. TMA Ecological Development Planning

The ecological development planning stages applied in the current work based on research background and applicable methods include the following items:

1. Calculate the probability of urbanization; 2. Identify the potential of ecological development and its overlap on the urbanization probability map; and 3. Extract naturally based protective barriers (green belt and green bows) and urban infill development potential. To reduce the destructive effects of future urban growth of TMA in the next 20 years using practical environmental policies such as reduction, reuse, and recycling of urban land uses with emphasis on infill development [65,66], nature conservation and natural landscapes, biodiversity in the urban landscape [67,68], and preservation of gardens and agricultural lands [69,70] around the TMA is essential. Therefore, through field study and analysis of future ecological development capacities and the policies mentioned above, we divided the policies into two strategies according to the ecologic approach for the new development area in the TMA. The detailed land use beside deteriorated textures of Tabriz provides useful potential that could be used under reduce, reuse, and recycle policy. The Tabriz metropolis has 702 hectares of inefficient land uses, including military barracks, small-scale pollutant industrial areas, warehouses and terminals incompatible with residential development, 420 hectares of deteriorated textures, 2462 hectares of one-story housing units in the form of increased building density, and 6043 hectares of vacant lands inside the Tabriz municipality district, which can assist in preserving the ecological green landscapes of Tabriz metropolis and restricting of urban sprawl over the next 20 years (Table 11 and Figure 10).

Table 11. Reduce, reuse, and recycle strategy.

City	Land-Use Type	Area (Ha)	Function
Tabriz	Incompatible land uses	702	Reducing environmental pollution
	Deteriorated textures	420	The revitalization of the city
	One-story housing units	2462	Infill development (compact city strategy)
	Vacant lands	6043	Limiting urban spatial polarization with the strengthening of new centers

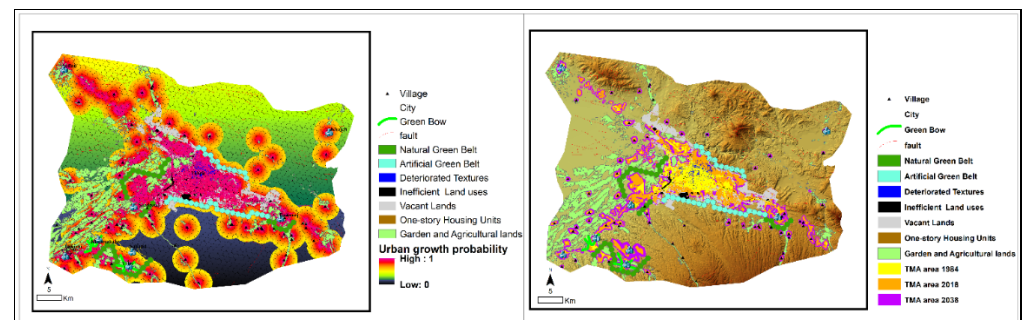


Figure 10. Left: extracting naturally based protective barriers (green belt and green bows) using hexagon blocking of the urban growth probability map for preservation of the ecological landscape in the TMA by 2038; right: simplified NB development in the TMA by 2038.

The second way to preserve other ecologically important cities, such as Basmenj, Sardroud, Khosroshahr, and Usko, is through the use of green belts and bows expansion. Therefore with hexagonal blocking of the urbanization probability map in the 1984–2018 period, LTM drove additional spatial agreement between the urban growth probability map and the built-up areas, considering the degree of resistance of land uses against ecological network development and providing required capacity for physical development for the cities of Khosroshahr and Usko, as well as nearby villages. Furthermore, green belts and green bows for ecological development were designed so that urban policymakers can use them to preventing the merging of towns and rural areas in the main body of the Tabriz metropolis (Table 12 and Figure 10).

Table 12. Proposed ecological green belt and bow policies for nature-based development.

City	Type	Direction	Length (Km)	Function
Tabriz	Artificial Green Belt	Northern	12.4	Stabilization of the urban development and limiting it toward the Tabriz fault
	Artificial Green Belt	Southern	21.3	Stabilization of the urban area and reducing air pollutants from industrial land use sources
	Natural Green Belt	Western	16.1	To preserve agricultural land and stop the spread of villages in the west of Tabriz
Basmenj	Natural Green Belt	Southern	6.3	Preservation of southern gardens of Basmenj
Sardroud	Natural Green Belt	Southern	4.4	Protection of southern gardens of Sardroud from rural development
Khosroshahr	Natural Green Belt	Eastern	4	Prevention of rural–urban integration in Khosrowshahr
	Natural green bow	Northern–Eastern	7.3	Preservation of garden lands in Khosrowshahr
Usko	Natural Green Belt	Eastern–Western–Southern	13.4	Prevention of rural–urban integration in Usko
	Natural green bow	Eastern–Western	6.4	Preservation of garden lands in Usko

3. Discussion and Conclusions

The landscape of the TMA experienced massive changes between 1984 and 2018, and this tendency will likely continue through 2038, driven by a rapid urban population growth rate. The aim of this study was to perform an analysis of the underlying factors of urban growth in the TMA, including their spatial patterns, using artificial neural network and logistic regression methods; to improve our understanding of the physical, environmental, and economic forces that have driven urban growth; and to identify the most probable sites for urban growth in the TMA. Both methods were implemented by running fifteen independent variables (selected through a literature review). The following independent factors affected urban growth in TMA more than other variables based on variation in ROC values: distance from urban centers, population density, urban CVN (center versus neighbor), slope, distance from roads, distance from CBDs, and distribution of land prices. Economic factors have played a significant role in the growth of the TMA. The study results show that urbanized areas have tripled within the last 34 years and seem likely to continue to increase. According to our results, natural/semi-natural areas (agricultural land and gardens) will be the first to be converted into urban land. In this study, to reduce the effect of spatial autocorrelation between simulated versus observed urban growth maps, we calculated the covariance of independent variables and put aside variables with correlation coefficients higher than 9.0, such as distance from administrative centers, distance from recreational centers, distance from cultural centers, distance from educational centers, and elevation. In the next section of the paper, from a practical perspective, we used the potential urban ecological principle that excites the boundary of the TMA with nature-based solutions to reduce costs for urban decision-makers to preserve agricultural and garden lands in the TMA over the next two decades. An efficient hybrid geospatial explicit method was developed by integrating a logistic regression model with the LTM model. The logistic regression model has the advantage of quantitatively exploring relationships between land conversion and causative factors, which enables distinguishing between effective variables [71]. However, simple logistic regression models are limited in several ways, such as in terms of determining when a change occurs, quantifying it, and ascribing it to different variables [59]. As a consequence, the present study was designed to rectify these constraints and to discover the interactions between various environmental and socioeconomic variables that lead to sprawl in urban areas. Several factors were assumed to contribute to urban growth in the study area (see Table 7). By examining ROC values, less effective variables were identified for consideration of the possible combination of variables in predicting urban growth.

These two techniques were combined for the following purposes. First, logistic regression and the LTM model were used to create a probability surface and to identify the most likely development sites and the amount of change. Secondly, the logistic regression model and the LTM model are powerful tools for ascertaining probable changes under predetermined population growth scenarios. The cells with the highest probability underwent the most change in these models. Therefore, these approaches can predict the most likely sites for development, estimate the likely amount of change, and distribute the estimated quantity within the study area. The logistic regression and LTM models have already been integrated and applied to various regions worldwide. We argue that combining these two approaches (i.e., logistic-LTM) offers certain advantages over traditional methods. As a first advantage, this approach can consider and integrate social and environmental factors that are not currently included in CA models, for example, SLUETH [72,73]. Secondly, any spatial factor can be included as part of this approach in order to measure its influence on urban sprawl and can be disregarded based on statistical analysis. As a final step, two methods of testing and verification were used: first, by measuring the ROC index and RMSE while the methodology was being developed and, second, by comparing the actual map to the simulated map of urbanization created to verify the methodology. Although the current LUCC models have frail approval, it is not conceivable to approve the certainty of the simulated maps in the longer term. Thus, the only way to guarantee a model's accuracy is to validate it within the most recent time period; after confirming the model's accuracy, future land-use maps can be simulated more confidently. In this study, we used the LTM module to address the weakness of logistic regression models that lack allocation processes. Our investigation also highlights the considerable limitations of this approach despite its strength. Although the proposed strategy can consolidate driving powers, it does join certain restrictions in parallel models, such as the non-factoring of individual conduct, individual inclinations, and legislative activities associated with use changes. In this research, we examined and predicted urban changes from the standpoint of urban ecosystem services, which regulate the relationship between urban development and the natural environment.

Author Contributions: Conceptualization, H.M.; methodology, A.A. and F.A.; software, F.A.; validation, A.A. and F.A.; formal analysis, H.M. and F.A.; investigation, H.M.; resources, A.A.; data curation, F.A.; writing—original draft preparation, H.M.; writing—review and editing, A.A. and F.A.; visualization, F.A.; supervision, H.M.; project administration, A.A.; funding acquisition, F.A. All authors have read and agreed to the published version of the manuscript.

Funding: This research received no external funding.

Institutional Review Board Statement: Not applicable.

Informed Consent Statement: Not applicable.

Data Availability Statement: Not applicable.

Conflicts of Interest: The authors declare no conflict of interest.

References

1. Gounaridis, D.; Chorianopoulos, I.; Symeonakis, E.; Koukoulas, S. A Random Forest-Cellular Automata modelling approach to explore future land use/cover change in Attica (Greece), under different socio-economic realities and scales. *Sci. Total Environ.* **2019**, *646*, 320–335. [[CrossRef](#)] [[PubMed](#)]
2. Vitousek, P.M.; Mooney, H.A.; Lubchenco, J.; Melillo, J.M. Human domination of Earth's ecosystems. *Science* **1997**, *277*, 494–499. [[CrossRef](#)]
3. Jiang, B.; Yao, X. *Geospatial Analysis and Modelling of Urban Structure and Dynamics*; Springer Science & Business Media: Berlin/Heidelberg, Germany, 2010; Volume 99.
4. Batisani, N.; Yarnal, B. Uncertainty awareness in urban sprawl simulations: Lessons from a small US metropolitan region. *Land Use Policy* **2009**, *26*, 178–185. [[CrossRef](#)]
5. Aguilar, R.; Cristóbal-Pérez, E.J.; Balvino-Olvera, F.J.; de Jesús Aguilar-Aguilar, M.; Aguirre-Acosta, N.; Ashworth, L.; Sanchez-Montoya, G. Habitat fragmentation reduces plant progeny quality: A global synthesis. *Ecol. Lett.* **2019**, *22*, 1163–1173. [[CrossRef](#)]
6. Andren, H. Effects of habitat fragmentation on birds and mammals in landscapes with different proportions of suitable habitat: A review. *Oikos* **1994**, *71*, 355–366. [[CrossRef](#)]
7. Fahrig, L. Effects of habitat fragmentation on biodiversity. *Annu. Rev. Ecol. Evol. Syst.* **2003**, *34*, 487–515. [[CrossRef](#)]
8. Haddad, N.M.; Brudvig, L.A.; Clobert, J.; Davies, K.F.; Gonzalez, A.; Holt, R.D.; Lovejoy, T.E.; Sexton, J.O.; Austin, M.P.; Collins, C.D.; et al. Habitat fragmentation and its lasting impact on Earth's ecosystems. *Sci. Adv.* **2015**, *1*, e1500052. [[CrossRef](#)]

9. Pauchard, A.; Aguayo, M.; Peña, E.; Urrutia, R. Multiple effects of urbanization on the biodiversity of developing countries: The case of a fast-growing metropolitan area (Concepción, Chile). *Biol. Conserv.* **2006**, *127*, 272–281. [[CrossRef](#)]
10. Seto, K.C.; Güneralp, B.; Hutyra, L.R. Global forecasts of urban expansion to 2030 and direct impacts on biodiversity and carbon pools. *Proc. Natl. Acad. Sci. USA* **2012**, *109*, 16083–16088. [[CrossRef](#)]
11. DeFries, R.S.; Rudel, T.; Uriarte, M.; Hansen, M. Deforestation driven by urban population growth and agricultural trade in the twenty-first century. *Nat. Geosci.* **2010**, *3*, 178. [[CrossRef](#)]
12. Li, G.; Lu, D.; Moran, E.; Calvi, M.F.; Dutra, L.V.; Batistella, M. Examining deforestation and agropasture dynamics along the Brazilian TransAmazon Highway using multitemporal Landsat imagery. *GIScience Remote Sens.* **2019**, *56*, 161–183. [[CrossRef](#)]
13. Musa, S.I.; Hashim, M.; Reba, M.N.M. Urban growth assessment and its impact on deforestation in Bauchi Metropolis, Nigeria using remote sensing and GIS techniques. *ARPN J. Eng. Appl. Sci.* **2017**, *12*, 1907–1914.
14. Romero, H.; Ihl, M.; Rivera, A.; Zalazar, P.; Azocar, P. Rapid urban growth, land-use changes and air pollution in Santiago, Chile. *Atmos. Environ.* **1999**, *33*, 4039–4047. [[CrossRef](#)]
15. Shao, M.; Tang, X.; Zhang, Y.; Li, W. City clusters in China: Air and surface water pollution. *Front. Ecol. Environ.* **2006**, *4*, 353–361. [[CrossRef](#)]
16. Song, Y.; Kirkwood, N.; Maksimović, Č.; Zhen, X.; O'Connor, D.; Jin, Y.; Hou, D. Nature based solutions for contaminated land remediation and brownfield redevelopment in cities: A review. *Sci. Total Environ.* **2019**, *663*, 568–579. [[CrossRef](#)]
17. Li, B.; Sivapalan, M.; Xu, X. An Urban socio-hydrologic model for exploration of Beijing's water sustainability challenges and solution spaces. *Water Resour. Res.* **2019**, *55*, 5918–5940. [[CrossRef](#)]
18. Walsh, C.J.; Fletcher, T.D.; Burns, M.J. Urban stormwater runoff: A new class of environmental flow problem. *PLoS ONE* **2012**, *7*, e45814. [[CrossRef](#)] [[PubMed](#)]
19. Morimoto, J.; Negishi, J. Ecological resilience of ecosystems to human impacts: Resilience of plants and animals. *Landsc. Ecol. Eng.* **2019**, *15*, 131–132. [[CrossRef](#)]
20. Parsons, A.W.; Rota, C.T.; Forrester, T.; Baker-Whetton, M.C.; McShea, W.J.; Schuttler, S.G.; Millsbaugh, J.J.; Kays, R. Urbanization focuses carnivore activity in remaining natural habitats, increasing species interactions. *J. Appl. Ecol.* **2019**, *56*, 1894–1904. [[CrossRef](#)]
21. Luo, M.; Lau, N.C. Urban expansion and drying climate in an urban agglomeration of east China. *Geophys. Res. Lett.* **2019**, *46*, 6868–6877. [[CrossRef](#)]
22. Mahmood, R.; Pielke Sr, R.A.; Hubbard, K.G.; Niyogi, D.; Dirmeyer, P.A.; McAlpine, C.; Carleton, A.M.; Hale, R.; Gameda, S.; Beltrán-Przekurat, A.; et al. Land cover changes and their biogeophysical effects on climate. *Int. J. Climatol.* **2014**, *34*, 929–953. [[CrossRef](#)]
23. Berberoğlu, S.; Akin, A.; Clarke, K.C. Cellular automata modeling approaches to forecast urban growth for Adana, Turkey: A comparative approach. *Landsc. Urban Plan.* **2016**, *153*, 11–27. [[CrossRef](#)]
24. Feng, Y.; Liu, Y.; Tong, X.; Liu, M.; Deng, S. Modeling dynamic urban growth using cellular automata and particle swarm optimization rules. *Landsc. Urban Plan.* **2011**, *102*, 188–196. [[CrossRef](#)]
25. Alghais, N.; Pullar, D. Modelling future impacts of urban development in Kuwait with the use of ABM and GIS. *Trans. GIS* **2018**, *22*, 20–42. [[CrossRef](#)]
26. Shirzadi Babakan, A.; Alimohammadi, A.; Taleai, M. An agent-based evaluation of impacts of transport developments on the modal shift in Tehran, Iran. *J. Dev. Eff.* **2015**, *7*, 230–251. [[CrossRef](#)]
27. Zhang, H.; Zeng, Y.; Bian, L.; Yu, X. Modelling urban expansion using a multi agent-based model in the city of Changsha. *J. Geogr. Sci.* **2010**, *20*, 540–556. [[CrossRef](#)]
28. Almeida, C.D.; Gleriani, J.; Castejon, E.F.; Soares-Filho, B.S. Using neural networks and cellular automata for modelling intra-urban land-use dynamics. *Int. J. Geogr. Inf. Sci.* **2008**, *22*, 943–963. [[CrossRef](#)]
29. Guan, Q.; Wang, L.; Clarke, K.C. An artificial-neural-network-based, constrained CA model for simulating urban growth. *Cartogr. Geogr. Inf. Sci.* **2005**, *32*, 369–380. [[CrossRef](#)]
30. Pijanowski, B.C.; Brown, D.G.; Shellito, B.A.; Manik, G.A. Using neural networks and GIS to forecast land use changes: A land transformation model. *Comput. Environ. Urban Syst.* **2002**, *26*, 553–575. [[CrossRef](#)]
31. Tayyebi, A.; Pijanowski, B.C.; Tayyebi, A.H. An urban growth boundary model using neural networks, GIS and radial parameterization: An application to Tehran, Iran. *Landsc. Urban Plan.* **2011**, *100*, 35–44. [[CrossRef](#)]
32. Thapa, R.B.; Murayama, Y. Scenario based urban growth allocation in Kathmandu Valley, Nepal. *Landsc. Urban Plan.* **2012**, *105*, 140–148. [[CrossRef](#)]
33. Hathout, S. The use of GIS for monitoring and predicting urban growth in East and West St Paul, Winnipeg, Manitoba, Canada. *J. Environ. Manag.* **2002**, *66*, 229–238. [[CrossRef](#)]
34. Hegazy, I.R.; Kaloop, M.R. Monitoring urban growth and land use change detection with GIS and remote sensing techniques in Daqahlia governorate Egypt. *Int. J. Sustain. Built Environ.* **2015**, *4*, 117–124. [[CrossRef](#)]
35. Moghadam, H.S.; Helbich, M. Spatiotemporal urbanization processes in the megacity of Mumbai, India: A Markov chains-cellular automata urban growth model. *Appl. Geogr.* **2013**, *40*, 140–149. [[CrossRef](#)]
36. Ozturk, D. Urban growth simulation of Atakum (Samsun, Turkey) using cellular automata-Markov chain and multi-layer perceptron-Markov chain models. *Remote Sens.* **2015**, *7*, 5918–5950. [[CrossRef](#)]

37. Tang, J.; Wang, L.; Yao, Z. Spatio-temporal urban landscape change analysis using the Markov chain model and a modified genetic algorithm. *Int. J. Remote Sens.* **2007**, *28*, 3255–3271. [[CrossRef](#)]
38. Huang, B.; Xie, C.; Tay, R.; Wu, B. Land-use-change modeling using unbalanced support-vector machines. *Environ. Plan. B Plan. Des.* **2009**, *36*, 398–416. [[CrossRef](#)]
39. Karimi, F.; Sultana, S.; Babakan, A.S.; Suthaharan, S. An enhanced support vector machine model for urban expansion prediction. *Comput. Environ. Urban Syst.* **2019**, *75*, 61–75. [[CrossRef](#)]
40. Mirbagheri, B.; Alimohammadi, A. Integration of local and global support vector machines to improve urban growth modelling. *ISPRS Int. J. Geo-Inf.* **2018**, *7*, 347. [[CrossRef](#)]
41. Rienow, A.; Goetzke, R. Supporting SLEUTH—Enhancing a cellular automaton with support vector machines for urban growth modeling. *Comput. Environ. Urban Syst.* **2015**, *49*, 66–81. [[CrossRef](#)]
42. Addae, B.; Oppelt, N. Land-use/land-cover change analysis and urban growth modelling in the Greater Accra Metropolitan Area (GAMA), Ghana. *Urban Sci.* **2019**, *3*, 26. [[CrossRef](#)]
43. Bekalo, M.T. Spatial Metrics and Landsat Data for Urban Landuse Change Detection: Case of Addis Ababa, Ethiopia. Doctoral Dissertation, Universitat Jaume I, Castellon, Spain, 2009.
44. Aarathi, A.D.; Gnanappazham, L. Comparison of urban growth modeling using deep belief and neural network based cellular automata model—A case study of Chennai Metropolitan area, Tamil Nadu, India. *J. Geogr. Inf. Syst.* **2019**, *11*, 1–16. [[CrossRef](#)]
45. Sejati, A.W.; Buchori, I.; Rudiarto, I. The spatio-temporal trends of urban growth and surface urban heat islands over two decades in the Semarang Metropolitan Region. *Sustain. Cities Soc.* **2019**, *46*, 101432. [[CrossRef](#)]
46. Wang, J.; Maduako, I.N. Spatio-temporal urban growth dynamics of Lagos Metropolitan Region of Nigeria based on Hybrid methods for LULC modeling and prediction. *Eur. J. Remote Sens.* **2018**, *51*, 251–265. [[CrossRef](#)]
47. Xia, C.; Zhang, A.; Wang, H.; Zhang, B. Modeling urban growth in a metropolitan area based on bidirectional flows, an improved gravitational field model, and partitioned cellular automata. *Int. J. Geogr. Inf. Sci.* **2019**, *33*, 877–899. [[CrossRef](#)]
48. Gong, J.; Hu, Z.; Chen, W.; Liu, Y.; Wang, J. Urban expansion dynamics and modes in metropolitan Guangzhou, China. *Land Use Policy* **2018**, *72*, 100–109. [[CrossRef](#)]
49. Siddiqui, A.; Siddiqui, A.; Maithani, S.; Jha, A.; Kumar, P.; Srivastav, S. Urban growth dynamics of an Indian metropolitan using CA Markov and Logistic Regression. *Egypt. J. Remote Sens. Space Sci.* **2018**, *21*, 229–236. [[CrossRef](#)]
50. Alaei Moghadam, S.; Karimi, M.; Habibi, K. Modelling urban growth incorporating spatial interactions between the cities: The example of the Tehran metropolitan region. *Environ. Plan. B Urban Anal. City Sci.* **2018**, *47*, 1047–1064. [[CrossRef](#)]
51. Sun, X.; Crittenden, J.C.; Li, F.; Lu, Z.; Dou, X. Urban expansion simulation and the spatio-temporal changes of ecosystem services, a case study in Atlanta Metropolitan area, USA. *Sci. Total Environ.* **2018**, *622*, 974–987. [[CrossRef](#)]
52. Pandey, B.; Joshi, P.; Singh, T.; Joshi, A. Modelling spatial patterns of urban growth in Pune Metropolitan Region, India. In *Applications and Challenges of Geospatial Technology*; Springer: Berlin/Heidelberg, Germany, 2019; pp. 181–203.
53. Thapa, R.B.; Murayama, Y. Urban growth modeling of Kathmandu metropolitan region, Nepal. *Comput. Environ. Urban Syst.* **2011**, *35*, 25–34. [[CrossRef](#)]
54. Puertas, O.L.; Henríquez, C.; Meza, F.J. Assessing spatial dynamics of urban growth using an integrated land use model. Application in Santiago Metropolitan Area, 2010–2045. *Land Use Policy* **2014**, *38*, 415–425. [[CrossRef](#)]
55. Hilbe, J.M. *Practical Guide to Logistic Regression*; Chapman and Hall/CRC: London, UK, 2016.
56. Li, J.; Dong, S.; Li, Y.; Li, Z.; Wang, J. Driving force analysis and scenario simulation of urban land expansion in Ningxia-Inner Mongolia area along the Yellow River. *J. Nat. Resour.* **2015**, *30*, 1472–1485.
57. Mahiny, A.S.; Turner, B.J. Modeling past vegetation change through remote sensing and GIS: A comparison of neural networks and logistic regression methods. In Proceedings of the 7th International Conference on Geocomputation, University of Southampton, Southampton, UK, 8–10 September 2003.
58. Hill, T.; Lewicki, P. *Statistics Methods and Applications*; StatSoft: Washington, DC, USA, 2007.
59. Hu, Z.; Lo, C. Modeling urban growth in Atlanta using logistic regression. *Comput. Environ. Urban Syst.* **2007**, *31*, 667–688. [[CrossRef](#)]
60. Aldrich, J.H.; Nelson, F.D.; Adler, E.S. *Linear Probability, Logit, and Probit Models*; Sage: Thousand Oaks, CA, USA, 1984.
61. Clark, W.; Hoskings, P. *Statistical Methods for Geographers*; John Wiley and Sons: New York, NY, USA, 1986.
62. Menard, S. *Applied Logistic Regression Analysis*; Sage: Thousand Oaks, CA, USA, 2002; Volume 106.
63. Xu, T.; Gao, J.; Coco, G. Simulation of urban expansion via integrating artificial neural network with Markov chain-cellular automata. *Int. J. Geogr. Inf. Sci.* **2019**, *33*, 1960–1983. [[CrossRef](#)]
64. Pijanowski, B.C.; Tayyebi, A.; Doucette, J.; Pekin, B.K.; Braun, D.; Plourde, J. A big data urban growth simulation at a national scale: Configuring the GIS and neural network based land transformation model to run in a high performance computing (HPC) environment. *Environ. Model. Softw.* **2014**, *51*, 250–268. [[CrossRef](#)]
65. Abedini, A.; Khalili, A. Determining the capacity infill development in growing metropolitans: A case study of Urmia city. *J. Urban Manag.* **2019**, *8*, 316–327. [[CrossRef](#)]
66. Adhvaryu, B.; Rathod, V. Estimating housing infill potential: Developing a case for floorspace pooling in Ahmedabad, India. *Plan. Pract. Res.* **2019**, *34*, 305–317. [[CrossRef](#)]
67. Heymans, A.; Breadsell, J.; Morrison, G.M.; Byrne, J.J.; Eon, C. Ecological urban planning and design: A systematic literature review. *Sustainability* **2019**, *11*, 3723. [[CrossRef](#)]

68. Warren-Kretschmar, B.; von Haaren, C. Design in landscape planning solutions. In *Landscape Planning with Ecosystem Services*; Springer: Berlin/Heidelberg, Germany, 2019; pp. 453–460.
69. Gyan, E. Green belt as a tool for containing urban sprawl: Exploring best practices in Germany. Book of Abstracts. In Proceedings of the 6th Fábos Conference on Landscape and Greenway Planning, Amherst, MA, USA, 29–30 March 2019.
70. Home, R.; Lewis, O.; Bauer, N.; Fliessbach, A.; Frey, D.; Lichtsteiner, S.; Moretti, M.; Tresch, S.; Young, C.; Zanetta, A.; et al. Effects of garden management practices, by different types of gardeners, on human wellbeing and ecological and soil sustainability in Swiss cities. *Urban Ecosyst.* **2019**, *22*, 189–199. [[CrossRef](#)]
71. Park, Y.S.; Lek, S. Artificial neural networks: Multilayer perceptron for ecological modeling. In *Developments in Environmental Modelling*; Elsevier: Amsterdam, The Netherlands, 2016; Volume 28, pp. 123–140.
72. Chaudhuri, G.; Clarke, K. The SLEUTH land use change model: A review. *Environ. Resour. Res.* **2013**, *1*, 88–105.
73. Eyelade, D.; Clarke, K.C.; Ijagbone, I. Impacts of spatiotemporal resolution and tiling on SLEUTH model calibration and forecasting for urban areas with unregulated growth patterns. *Int. J. Geogr. Inf. Sci.* **2022**, *36*, 1037–1058. [[CrossRef](#)]